NUCLEAR ASTROPHYSICS
AND THE DARESBURY RECOIL SEPARATOR
AT THE HOLIFIELD RADIOACTIVE ION BEAM FACILITY

M. S. SMITH

Physics Division, Oak Ridge National Laboratory,
MS-6354, Bldg. 6010, P.O. Box 2008,
Oak Ridge, TN 37831-6371, USA

The Daresbury Recoil Separator (DRS) has been installed for nuclear astrophysics research at Oak Ridge National Laboratory's Holifield Radioactive Ion Beam Facility. It will be used for direct measurements of capture reactions on radioactive ions which occur in stellar explosions such as novae, supernovae, and X-ray bursts. These measurements will be made in inverse kinematics with radioactive heavy ion beams incident on hydrogen and helium targets, and the DRS will separate the capture reaction recoils from the intense flux of beam particles. Details of the new DRS experimental equipment and preliminary results from the first commissioning experiments with stable beams are described, along with the plans for the first measurements with radioactive beams. Other astrophysics research efforts at ORNL - in theoretical astrophysics, nuclear astrophysics data evaluation, heavy element nucleosynthesis, theoretical atomic astrophysics, and atomic astrophysics data - are also briefly described.

1 Introduction

1.1 Physics Motivation

There are a number of very important and exotic astrophysical events during which hydrogen serves as fuel for (p, γ) fusion reactions (i.e., is burned) under non-hydrostatic equilibrium conditions. These explosive hydrogen burning events, which include novae, supernovae, and X-ray bursts, are among the most energetic explosions ($\sim 10^{40-51}$ ergs) known in the universe. Furthermore, novae and supernovae are among the primary sources of the elements heavier than lithium. For this reason, they have been the focus of intense scientific research including astrophysical observations using new devices such as the Compton Gamma Ray Observatory and the Hubble Space Telescope, theoretical modeling of explosions utilizing massively parallel supercomputers, and laboratory measurements of the nuclear reactions that occur in (and sometimes drive) the explosions. These catastrophic stellar events are characterized by extremely high temperatures (10^{8-9} K) and densities (10^{3-6} g/cm^3), conditions which cause (p, γ) reactions to rapidly (on timescales of ns - min) produce nuclei on the proton-rich side of the valley of stability. Any such nuclei (which decay via e^+-emission or e^--capture) produced

1

DISCLAIMER

with half-lives longer than, or comparable to, the mean time between fusion events will become targets for subsequent nuclear reactions. Sequences of (p, γ) reactions on *proton-rich radioactive nuclei* can therefore occur during these explosions [1], and the observable ashes of such nuclear burning sequences are an important probe of the conditions (temperatures, densities, timescales) in these events. Critical comparisons of astrophysical models with the latest observations require measurements of these crucial reactions involving radioactive isotopes. Such measurements have been, until recently, impossible because of the lack of intense radioactive nuclear beams. Explosion models therefore employ reaction rate estimates based on systematic properties of nuclear states, on information from analogue nuclei, on partial resonance information from stable beam transfer reaction studies, and on statistical model calculations. Such rate estimates can, however, be incorrect by orders of magnitude [2], and therefore the model predictions of isotope synthesis and energy generation are necessarily incomplete. The recent development of ^{13}N, ^{19}Ne, and ^{18}F radioactive beams at Louvain-la-Neuve and their use in measuring the astrophysically important reactions $^{13}N(p,\gamma)^{14}O$ [3], $^{19}Ne(p,\gamma)^{20}Na$ [4], and $^{18}F(p,\alpha)^{15}O$ [5, 6], as well as the measurement of $^{18}F(p,\alpha)^{15}O$ at Argonne National Lab [7], has initiated a new era in laboratory nuclear astrophysics – one in which crucial, previously unattainable nuclear cross sections can be measured and subsequently incorporated into an emerging generation of sophisticated, computationally intensive models of stellar explosions. By producing high-quality, intense beams of the radioactive ions that play a crucial role in explosive nucleosynthesis, the Holifield Radioactive Ion Beam Facility (HRIBF) at ORNL has the potential to significantly improve the understanding of these spectacular stellar explosions.

1.2 Important Nuclear Reactions

There is a strong overlap between the radioactive ion beams that are anticipated at the HRIBF and those radioactive nuclei involved in explosive hydrogen burning reactions occurring in hot, dense stellar environments. Reactions that will be studied with HRIBF beams include those in the Hot CNO cycle [8], occurring at stellar temperatures $T_9 \approx 0.1 - 0.2$ [where $T_9 \equiv T\,(K)\,/\,10^9$] in red giants, nova explosions, and supermassive stars. Additionally, reactions in sequences such as $^{14}O(\alpha,p)^{17}F(p,\gamma)^{18}Ne(e^+\nu_e)^{18}F(p,\gamma)^{19}Ne(p,\gamma)^{20}Na(p,\gamma)^{21}Mg..$ will be accessible at the HRIBF, as will the $^{15}O(\alpha,\gamma)^{19}Ne(p,\gamma)^{20}Na(p,\gamma)^{21}Mg...$ sequence. At $T_9 \approx 0.4$, these may process C, N, and O nuclei to masses $A > 20$, therefore leading to hydrogen burning through the rapid proton capture process (rp-process). [1] These "breakout" reaction sequences can increase the energy generated through nuclear burning, and significantly alter the abundances produced during stellar explosions.

2

HRIBF beams will also enable studies of rp-process reactions, thought to occur at higher temperatures ($T_9 > 0.4$) characteristic both of the most energetic novae and of X-ray bursts. The rp-process path involves (p, γ) reactions near the proton drip line competing with e^+ - decay and reaction cycles (e.g., the Ne-Na and Mg-Al cycles); the process may produce nuclei up to mass 56 or, at temperatures $T_9 > 1$, even up to masses 70 - 100. Detailed calculations of the element synthesis and energy generation in the rp-process have recently been made. [9, 10] Because almost all relevant reactions in the Hot CNO breakout and in the rp-process are *unmeasured*, and because these sequences are sensitive to many of these rates, current calculations of these paths may be fundamentally altered with direct measurements of crucial reaction rates and other important nuclear parameters. Better reaction rates will also help determine the onset of the rp-process, the termination of the rp-process, and (in some cases) the temperatures of stellar explosions by comparison to abundance observations (e.g., for Mg and Al isotopes [11]).

1.3 Initial Radioactive Ion Beam Measurements at HRIBF

Some of the first astrophysically important radioactive ion beams anticipated at the HRIBF include ^{17,18}F, ^{56}Ni, and ^{7}Be. A brief description of each of the planned initial HRIBF measurements with these beams is given in the following subsections. Details of the experimental techniques and apparatus are given in Section 3.

1.3.1 The $^{14}O(\alpha, p)^{17}F$ Reaction

This reaction initiates the sequence $^{14}O(\alpha,p)^{17}F(p,\gamma)^{18}Ne(e^+ \nu_e)^{18}F(p,\alpha)^{15}O$ that, at high temperatures ($\sim 10^8$ - 10^9 K) and densities ($\sim 10^3$ - 10^6 g/cm^3), can bypass the slow (compared to the explosion timescale) ^{14}O positron decay in the Hot CNO cycle [$^{12}C(p,\gamma)^{13}N(p,\gamma)^{14}O(e^+ \nu_e)^{14}N(p,\gamma)^{15}O(e^+ \nu_e)^{15}N(p,\alpha)^{12}C$]. This bypass increases the energy generation rate and changes the abundances of isotopes produced in these explosions. As mentioned above, the reaction sequence $^{14}O(\alpha, p)^{17}F(p, \gamma)^{18}Ne(e^+ \nu_e)^{18}F(p, \gamma)^{19}Ne(p, \gamma)^{20}Na(p, \gamma)^{21}Mg...$ serves at high temperatures as a transition or "breakout" from the stellar catalytic Hot CNO cycle to the rapid proton capture- (rp-) process. [1, 2] Even a small branch through this reaction sequence can result in substantial buildup of elements heavier than mass 20 that cannot be formed in the Hot CNO cycle, but that are observed in remnants of stellar explosions. [12, 13] The rate for the $^{14}O(\alpha,p)^{17}F$ reaction is quite uncertain, however, because of the unknown properties (Γ_α and Γ_{tot}) of the $E_x = 4.561$ MeV level in ^{18}Ne that possibly dominates the reaction at explosive hydrogen burning temperatures [14]; there are additional uncertainties in higher energy resonances

3

that will contribute at stellar temperatures $T_9 > 1$. It is planned to measure the inverse of this reaction, $^{17}F(p,\alpha)^{14}O$, at HRIBF, with a radioactive ^{17}F beam and a hydrogen (CH_2) target. The inverse reaction was chosen for a number of reasons: the higher energy of the exiting alpha particles makes them easier to detect than the protons from the forward reaction; the forward focussing of the alphas in the laboratory frame makes a high detection efficiency possible; and hydrogen (in the form of CH_2 foils) is a more readily available target than He. A ^{17}F beam intensity of 10^{6-7} s^{-1} is required for this measurement.

1.3.2 The $^{17}F(p,\gamma)^{18}Ne$ Reaction

This reaction is part of the Hot CNO breakout reaction sequence initiated by $^{14}O(\alpha,p)^{17}F$ described in the previous subsection. Additionally, $^{17}F(p,\gamma)^{18}Ne$ plays an important role in the sequence $^{16}O(p,\gamma)^{17}F(p,\gamma)^{18}Ne(e^+\nu_e)^{18}F$, which alters the $^{17}O/^{18}O$ abundance ratio – a stable-isotope tracer of Hot CNO cycle burning. This sequence, which occurs independently of a Hot CNO breakout, also alters the abundance of ^{18}F, a radioisotope that is a candidate for gamma-ray observations in the interstellar medium. [15] For these reasons, it is important to determine the $^{17}F(p,\gamma)^{18}Ne$ rate at temperatures characteristic of stellar explosions. It is planned to first measure the $^{17}F(p,p)^{17}F$ excitation function at the HRIBF to confirm the presence of a (p,γ) resonance at $E_x = 4.561$ MeV in ^{18}Ne that possibly dominates the reaction rate at nova temperatures. This resonance has been observed in a measurement of the $^{16}O(^3He,n)^{18}Ne$ reaction [16], but has not been observed in measurements of the $^{20}Ne(p,t)^{18}Ne$ reaction. [14, 17] From comparison to the isobaric analog nucleus ^{18}O, this resonance may have $J^\pi = 3^+$, which potentially makes it a very strong $\ell = 0$ transition in the $^{17}F(p,\gamma)^{18}Ne$ reaction. The $^{17}F(p,\gamma)^{18}Ne$ capture reaction itself – with a cross section $\approx 2.5\,\mu b$ – is too weak to be used to search for the resonance. The stronger (p,p) reaction will therefore be used to verify the existence of and determine the energy of this state, as well as to set limits on its spin and parity. Then, the absolute resonant $^{17}F(p,\gamma)^{18}Ne$ cross section will be measured to directly determine the resonant contribution to the (p,γ) reaction rate. An 11.5 MeV ^{17}F beam of intensity of $1 \cdot 10^5$ s^{-1} is required to measure the $^{17}F(p,p)^{17}F$ excitation function. For $^{17}F(p,\gamma)^{18}Ne$, an intensity of approximately $6 \cdot 10^7$ s^{-1} (0.01 pnA) would be required to make a 10 % measurement in 25 days at the dominant resonance, whereas a 3 % measurement can be made in three weeks of beam time with a ^{17}F beam intensity of 0.1 pnA.

1.3.3 The $^{18}F(p,\alpha)^{15}O$ and $^{18}F(p,\gamma)^{19}Ne$ Reactions

The branching ratio between the $^{18}F(p,\alpha)^{15}O$ and the $^{18}F(p,\gamma)^{19}Ne$ reactions

determines if the sequence $^{14}O(\alpha,p)^{17}F(p,\gamma)^{18}Ne(e^+\nu_e)^{18}F$ serves only to bypass the ^{14}O beta decay, or if it serves to process C, N, and O seed nuclei out of the Hot CNO cycle and into the rp-process. The rates of these two competing reactions are determined by the properties of the resonances in the ^{19}Ne compound nucleus just above the $^{18}F + p$ threshold. Recent stable-beam nuclear spectroscopy measurements [18, 19, 20] suggest that the resonances at $E_{cm} = 330$ and 659 keV (corresponding to ^{19}Ne excited states at $E_x = 6.741$ and 7.070 MeV, respectively) are the most important resonances for these two reactions at nova and X-ray burst temperatures. However, the spin, parity, and Γ_γ of the 659-keV resonance are unknown, and the Γ_p of the 330-keV resonance is unknown. These partial widths or resonance strengths, estimates of which can be in error by an order of magnitude, need to be determined by radioactive ion beam experiments. Recently, low-intensity ^{18}F radioactive beams of intensities $\leq 10^6$ s^{-1} have been used at Louvain-la-Neuve [5, 6] and Argonne National Laboratory [7] to study $^{18}F(p,\alpha)^{15}O$. At HRIBF, it is first planned to use a low-intensity ($\approx 10^5$ s^{-1}) ^{18}F radioactive ion beam to measure excitation functions and angular distributions for the $^{18}F(p,p)^{18}F$ reaction to help determine the spin and parity for the $E_{cm} = 659$ keV resonance. Next, it is planned to directly measure the $^{18}F(p,\alpha)^{15}O$ cross section on both resonances to determine their resonance strengths, and to improve the resolution and statistics of the previous (p, α) measurements and resolve their differences. Finally, it is planned to directly measure the strengths of these resonances for the $^{18}F(p,\gamma)^{19}Ne$ reaction at HRIBF. These latter two measurements will require an ^{18}F beam intensity of $6 \cdot 10^6$ s^{-1} and $6 \cdot 10^7$ s^{-1}, respectively.

1.3.4 The $^{56}Ni(p,\gamma)^{57}Cu$ Reaction

The $^{56}Ni(p,\gamma)^{57}Cu$ reaction is an important link in the synthesis of elements heavier than Ni via very high temperature ($T_9 > 1$) explosive hydrogen burning that occurs in X-ray bursts. [10] Reaction rates derived from two recent studies -- one employing a stable beam to populate important resonances in ^{57}Cu [21], the other employing a radioactive ^{56}Ni beam and the (d,p) reaction to populate analogue states in ^{57}Ni [22] -- differ by a factor of 10. A measurement of the $^{56}Ni(p,p)^{56}Ni$ elastic scattering excitation function is planned at the HRIBF to improve the determination of the stellar $^{56}Ni(p,\gamma)^{57}Cu$ reaction rate and resolve the differences of the two recent studies. Excitation energies and total widths will be measured, and limits on the spins and parities will be set, of ^{57}Cu resonances above the $^{56}N + p$ threshold that dominate the $^{56}Ni(p,\gamma)^{57}Cu$ reaction rate. A 56 MeV ^{56}Ni beam of minimum intensity of 10^5 s^{-1} is required for this measurement. The information from the (p,p) measurement will be used both for an improved reaction rate calculation and as a basis for a future absolute cross section measurement of

^{56}Ni(p,γ)^{57}Cu at the HRIBF when a sufficient radioactive beam intensity (6 • 10^8 s^{-1}) is available.

1.3.5 The ^{7}Be(p,γ)^{8}B Reaction

The current 25 % uncertainty in the cross section (or astrophysical S-factor) of the ^{7}Be(p,γ)^{8}B reaction [23 - 25] is the largest of any solar thermonuclear reaction, and corresponds to more than half of the total uncertainty in the predicted solar neutrino capture rates [25] of the Homestake (^{37}Cl) and Kamiokande solar neutrino detectors. While a new measurement of S_{17} will not solve the "solar neutrino problem" – the persistent factor of 2 to 4 discrepancy between the measured and predicted capture rates of solar neutrinos – it could significantly reduce the largest remaining nuclear physics uncertainty in the calculation of predicted neutrino capture rates. Accurate capture rate calculations will be especially important for interpreting the results anticipated from a new generation of solar neutrino detectors (e.g., the Sudbury Neutrino Observatory) that will give detailed information on the ν energy spectrum.

Both the absolute magnitude of S_{17} (over the measured energy range E_{cm} = 0.2 - 1.0 MeV) [24] and its theoretical extrapolation to stellar energies (E_{cm} ≈ 0.01 MeV) [23, 26] are the focus of international scientific attention. The planned HRIBF experiment will focus on measuring the absolute magnitude of S_{17} using a radioactive ^{7}Be beam (at E_{cm} = 0.5 and 1.0 MeV) incident on a hydrogen windowless gas-cell target. This measurement will be independent of the radioactive ^{7}Be target thickness uncertainties affecting all of the earlier measurements (except the recent measurement utilizing the Coulomb dissociation of ^{8}B [27]). The expected yield of this reaction is 470 day^{-1}, assuming a ^{7}Be beam current of 0.35 pnA (2 • 10^9 s^{-1}), a cross section of 500 nb (at E_{cm} = 1.0 MeV), and a hydrogen gas target thickness of 5 • 10^{18} cm^{-2}. In four days of beam time, 3 % statistics can be attained. At E_{cm} = 0.5 MeV, the ^{7}Be(p,γ)^{8}B cross section (and therefore the yield) is lower by a factor of 2.5.

2 The Holifield Radioactive Ion Beam Facility

2.1 Radioactive Beam Production

The Holifield Radioactive Ion Beam facility [28, 29] is the only U.S. facility able to produce and accelerate beams of proton-rich radioactive heavy ions. The first experiment with a radioactive ion beam at this user facility was completed in Spring 1997. [30] Radioactive ions are produced when a high-temperature (1100 - 2200° C), thin, refractory target [31, 32] is bombarded by a 0.5 kW light ion (p, d,

^{3}He, or ^{4}He) beam from the K=105 Oak Ridge Isochronous Cyclotron (ORIC); the ORIC beam power will eventually be increased to 2 kW, giving larger yields of radioactive ions. For example, fibrous Al_2O_3 targets [33] (with a high surface area to volume ratio and low density to enhance diffusion of radioactive isotopes) are being used to produce ^{17}F via the ^{16}O(d, n)^{17}F reaction at 30 MeV. A number of novel target configurations for high-efficiency release of radioactive isotopes are currently under design. [32] Once produced by transfer or evaporation reactions induced by ORIC beams, the radioactive isotopes diffuse out of the hot target material and through a short (10 cm) transfer tube to a modular (i.e., changeable) ion source for ionization and extraction. Ion sources are being developed to maximize the extracted radioactive beam. Currently an electron beam plasma ion source [32] is used for radioactive beams of As, Ga, and F, and a positive/negative surface ionization source has been developed for producing negative ions of radioactive fluorine. [34] A number of other ion sources are under development, including a thermal dissociator/electron impact ion source [35] and a large-plasma-volume, compact, multi-frequency ECR ion source. [36] Once produced, the radioactive ions are then charge-exchanged (if they are positive ions) in a Cs vapor cell, then undergo two stages of mass separation (with $\Delta M / M \leq 0.5 - 1 \cdot 10^{-4}$) before their injection into the 25-MV tandem accelerator and their subsequent acceleration and delivery to the experimental areas.

To date, radioactive beams of ^{69,70}As and ^{66,67}Ga suitable for experiments have been produced at the HRIBF; the ^{69}As beam was used for the first HRIBF experiment [30] in nuclear structure physics and had an intensity 10^6 s^{-1} on target. The ^{69}As beam was produced by (p,2n) reactions on a liquid Ge target heated to 1300° C. An electron beam plasma ion source ionized the products. The efficiency of the target/ion source system was measured at the UNISOR isotope separator (with a low-intensity proton beam bombardment) to be 0.5 % with a hold up time of 3.6 hours. [37] Radioactive ^{17,18}F beams are needed for astrophysics experiments, and low-intensity fluorine beams have been produced at UNISOR with the fibrous Al_2O_3 target mentioned above. The efficiency was 0.005 % (for the molecular species Al^{17}F$^+$) and 0.06 % (for Al^{18}F$^+$) with a hold up time of 16.4 minutes. [37] These measurements used an electron beam plasma ion source – which is known to have a low efficiency for F ions. The 0.005 % efficiency corresponds to, for example, a ^{17}F beam intensity of approximately 10^6 s^{-1} when scaled up to the higher-intensity (10 μA) deuterons that will be used from ORIC. However, the charge-exchange efficiency will be only a few percent for this beam, which will significantly reduce the beam available for experiments. Additional fluorine target/ion source tests with low- and high-intensity light-ion bombardment are continuing. A new surface ionization source has produced (stable) F$^-$ ions with a

7

1–4 % efficiency [38] which needs no charge exchange, and therefore promises to substantially improve the yield of radioactive fluorine ions over that from an electron beam plasma ion source.

While proton-rich radioactive isotopes are currently being produced at the HRIBF, tests will soon begin on using a uranium carbide target to produce neutron-rich radioactive isotopes. This will enable studies in heavy element nucleosynthesis, described briefly in Section 4.3.

2.2 HRIBF Beam Quality

Radioactive ion beams produced at the HRIBF have a number of important characteristics which make them well suited for nuclear astrophysics studies: high isobaric purity, good energy resolution, low emittance, low energies, and relatively high intensities. The importance of some of these characteristics are discussed in detail in ref. [39]. The HRIBF two-stage mass analysis system on the tandem accelerator injector line gives a very high isobaric purity ($\Delta M / M \leq 0.5 - 1.0 \cdot 10^{-4}$), substantially reducing backgrounds from capture reactions on stable isobars. The tandem accelerator has excellent energy resolution ($\Delta E / E \leq 10^{-4}$) and emittance (0.5 π mm·mrad), both important for high-precision, low-background absolute cross section measurements. Furthermore, the tandem efficiency at the low terminal potentials corresponding to astrophysically important energies ($E / A = 0.2 - 2$ MeV/u) has recently been improved by replacing the accelerating column spark gaps by a resistor chain. Finally, the radioactive beam intensities will vary greatly with the species, but the anticipated values are $10^6 - 10^{10}$ s^{-1} [28, 29], sufficient for a variety of nuclear astrophysics measurements.

3 Experimental Techniques and Apparatus

3.1 Direct Measurements of Capture Reactions

Nuclear astrophysics experiments at the HRIBF will focus on absolute cross section measurements of astrophysically important capture reactions on radioactive nuclei in inverse kinematics – that is, a heavy radioactive ion beam incident on a hydrogen target, such as p(^{17}F, ^{18}Ne)γ. These measurements will utilize a recoil separator for direct recoil detection, which has a number of advantages over more traditional capture γ ray detection techniques. [40] The most important advantage is the high detection efficiency possible with a device of moderate acceptance, because of the forward focusing of the recoils in the laboratory frame: all recoils are within a 0.5° opening angle of the beam direction. Other advantages include a significant increase in the signal-to-noise ratio, because the detectors are placed far from the

8

high radiation area near the target, and an increase in the detection schemes possible at the focal plane of a recoil separator – such as direct recoil detection, delayed-activity detection, and recoil-γ coincidences. The recoil detection approach is, however, very challenging because: (1) the projectiles and recoils differ in angle by only 0.5°, so the separator must be located along the beam axis and therefore accept *all* of the beam particles; (2) the recoils are only 10^{-10} to 10^{-12} times as intense as the projectiles; and (3) the projectiles and recoils are "nearly" identical: they have approximately the same momentum, and differ in velocity by only a few percent and in mass by only one amu. It is therefore necessary to optimize the recoil separator to collect one mass group (the recoils) at the final focus with the highest possible (10^{-10} to 10^{-12}) suppression of scattered projectiles. It is also necessary to instrument the final focus of the separator with detectors designed to distinguish between the scattered projectiles and recoils, which is quite challenging in view of the low-energy (0.4 - 2 MeV/u) and low-mass of the particles to be identified. The recoil detection technique for proton capture reactions was first proven viable with a measurement of the $p(^{12}C,^{13}N)\gamma$ reaction with a relatively small, non-optimized recoil separator at Caltech [40], where a 10^{-10} suppression of scattered beam particles was obtained.

The Daresbury Recoil Separator (DRS), built for a nuclear structure research program at Daresbury Laboratory in the U.K. [41], was transferred to the HRIBF where it forms the core of an endstation dedicated for nuclear astrophysics capture reaction measurements. The DRS is installed and is currently being commissioned with stable beams, described in Section 3.2. The device, shown in Figure 1, is a large-acceptance (6.5 msr, ± 2.5 % in velocity), high-mass resolution (300), 90-ton, 13 meter-long mass separator that was designed to detect weak channels in fusion evaporation reactions — where there is typically a large velocity difference between the beam particles and the recoils of interest. The DRS features two long (1.2 meter), crossed electric and magnetic field velocity filters, followed by a 50° dipole magnet that gives a mass/charge final focus. There are 14 magnets in total: two velocity filter dipoles, 9 quadrupoles, two sextupoles, and the 50° dipole. The velocity filters have maximum electric and magnetic field strengths of approximately 4 MV/m and 0.5 Tesla, respectively. To increase the projectile suppression of the DRS for inverse-kinematics proton capture reactions at the HRIBF, the system has been configured to have an ion-optic focus and adjustable slits between the two velocity filters. This arrangement effectively decouples the two velocity filters – they are now operated as separate spectrometers. The majority of the projectiles are stopped in the new slits between the two velocity filters. In another change, the velocity filters now have opposite field orientations (and therefore opposite deflections of the beam particles), a configuration estimated by ion - optics calculations to give the best projectile suppression. Monte Carlo
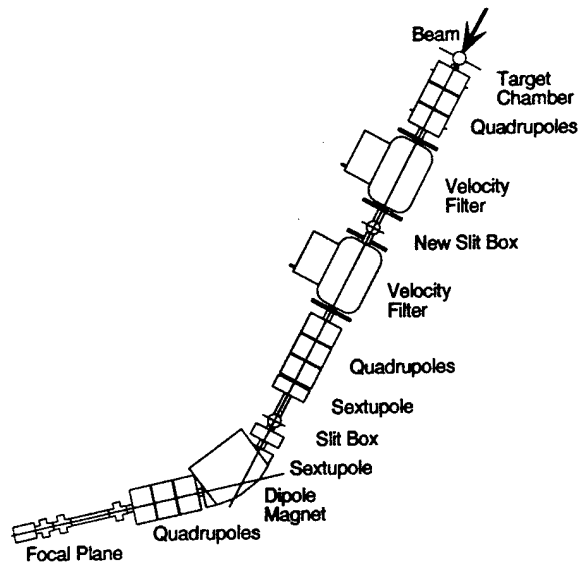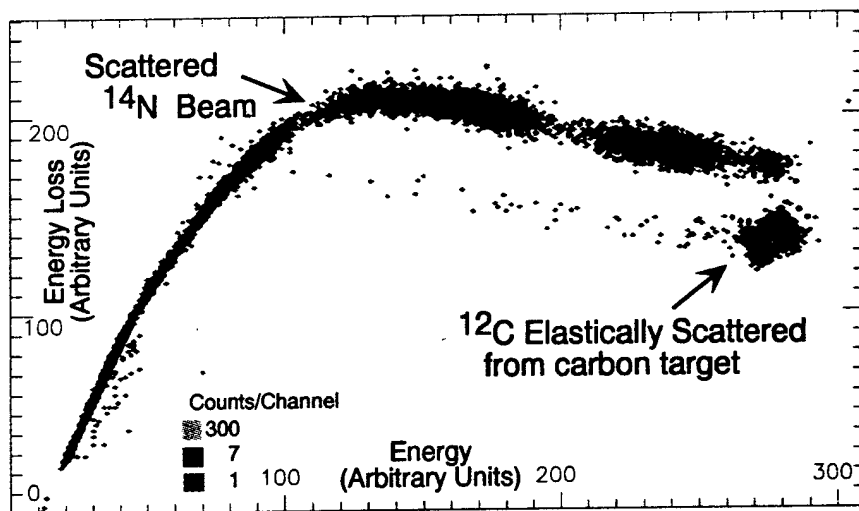
Figure 1: The Daresbury Recoil Separator

Figure 2. DRS Focal Plane Ion Counter Elastic Scattering Spectrum

10

simulations have been performed to determine the placement of slits to minimize the scattered beam that is estimated to reach the focal plane. Detailed focusing adjustments in the form of linear combinations of field strengths of the 14 DRS magnets have been determined for some of the most common aberrations. [42] In another modification, the distance between the final DRS quadrupole and the focal plane has been increased to accommodate the future installation of two timing detectors separated by 1.5 meters. The time-of-flight difference between projectiles and recoils will be used for improving projectile suppression. A new compact target chamber has also been constructed for the DRS, designed so that a highly-segmented BaF_2 array can be placed close to the target for the detection of capture γ rays. A second target chamber, described in Section 3.3, has been built for (p,p) and (p,α) measurements. Both of these chambers will accommodate CH_2 foil targets as the source of hydrogen; initial experiments will be run with these targets because of their ease of fabrication, whereas later experiments will use a gas target (described below). The DRS transmission of capture-reaction recoils is limited primarily by the charge-state selectivity of the 50° dipole magnet to be approximately 40 % for many of the recoils of interest. This high efficiency enables measurements of resonant (p, γ) cross sections as low as ~1 μb (corresponding to resonance strengths ~1 meV [8]) with 3 % statistics to be made in approximately 3 weeks with radioactive beam intensities of 0.1 pnA ($6 \cdot 10^8$ s^{-1}) and thick targets.

There are two detectors currently operating at the DRS focal plane: a carbon-foil microchannel plate detector (providing timing and position information) and a gas ionization counter (providing particle identification). The first detector has an intrinsic horizontal position resolution of 1 mm, as tested with radioactive sources and slits at the HRIBF. This is sufficient because the target-to-detector DRS horizontal magnification is approximately a factor of 3 and the target beam spot width is approximately equal to 1 mm. The ion counter has three separate anodes for particle identification – two energy loss signals and one residual energy signal – and is typically operated with 5 - 30 torr of isobutane gas. Details of the detectors can be found in ref. [41]. The performance of the ion counter for the low-mass, low-energy ions of interest is discussed in Section 3.2.

Future DRS detector systems include a second carbon-foil microchannel plate detector (for timing, as mentioned above) and a moving tape system with associated NaI detectors for delayed activity measurements. A windowless, differentially-pumped gas cell target, and a gas jet target, are currently being designed for the DRS. The design of the cell is similar to that used in Naples. [43] Gas targets are preferred over CH_2 foil targets for a number of reasons. Higher yields are obtained for the same target (energy loss) thickness, since there is no energy loss to carbon

11

atoms in the gas target. Also, alpha-induced reactions $[(\alpha, \gamma)$ and $(\alpha, p)]$ are measurable with gaseous helium targets. Finally, the background from carbon-induced reactions is greatly reduced when pure gas targets are used, and gas targets have no physical degradation or hydrogen-depletion problems common to CH_2 foils.

3.2 Commissioning Experiments

Commissioning of the DRS began in the summer of 1997 with radioactive sources and with stable beams. The $^{14}N + {}^{12}C$ elastic scattering reaction was recently measured with a 1 MeV/u ^{14}N beam and a carbon target as a first simulation of the projectile rejection of the DRS for radiative capture reactions on low-energy, low-mass, radioactive ion beams – see Figure 2. The DRS was tuned for the ^{12}C particles knocked out of the target by the beam, and the suppression of the scattered beam particles – defined by the ratio of beam particles incident on target to those reaching the focal plane – was measured to be $5 \cdot 10^{-11}$, within the 10^{-10} to 10^{-12} range needed. Furthermore, as shown in Figure 2, the gas ionization counter cleanly separated (i.e., with no overlap) the energy-loss (i.e., Bragg) curves of the low-mass, low-energy carbon and nitrogen particles above 0.4 MeV/u. In this first test, the combined projectile rejection of the DRS and the focal plane detector was well beyond that needed for capture reactions. The one-unit difference in nuclear charge between beam and recoils was the same in this elastic scattering simulation as in a radiative capture reaction, as was the low energy and mass of the ions. Since the elastic scattering has a factor of 10^6 larger cross section and a larger recoil angular spread, the DRS projectile suppression could be different for radiative capture reactions. However, a recently-performed second test shows that this is not the case: the $p(^{12}C, {}^{13}N)\gamma$ reaction was measured with a 0.666 MeV/u ^{12}C beam and a CH_2 target in a true test of the DRS projectile suppression. The preliminary determination of the suppression of scattered beam particles was $3 \cdot 10^{-11}$, agreeing with the elastic scattering results, and the ^{13}N recoils were cleanly separated from the scattered ^{12}C projectiles in the ionization counter. Further commissioning tests are planned to optimize these results and to determine the DRS transmission.

3.3 Other Nuclear Astrophysics Measurements

In addition to (p, γ) capture reaction studies, other types of nuclear astrophysics measurements are planned with HRIBF's accelerated beams of proton-rich radioactive heavy ions. Reactions such as (p, p) and (p, α) with radioactive beams in inverse-kinematics (e.g., $p(^{17}F, {}^{17}F)p$) will be used to precisely determine resonance energies, total widths, limits on spins and parities, and cross sections (see

12

Section 1.3). Once a He gas target is available, (α, p) reactions will be measured with the same techniques. Light-ion products of these reactions will be detected in a silicon detector array (SIDAR), an annular array of 128 silicon strip detectors similar to the array in ref. [44]. A large (40 cm diameter) chamber has been built to house this array. The solid angle coverage is approximately 25 % – and this corresponds to an even higher detection efficiency for some reactions because of the kinematic focussing of the light ions. Because the (p, p) scattering cross sections are ~1 b, low radioactive ion beam intensities (~10^5 s^{-1}) can be utilized for these measurements. With thin targets (10^{17} cm^{-2}) and a 25 % detector efficiency, 3% statistics for the total cross section can be obtained in one day; longer periods are required for angular distribution and excitation function measurements. The cross sections for (p, α) reactions are lower than for (p, p), but are still ~ 10^2 - 10^3 larger than the corresponding (p, γ) cross sections. For example, 10 % counting statistics can be obtained in each silicon strip detector in ten hours with a beam current of ~10^6 s^{-1} for one resonance in the p(^{17}F, ^{14}O)α reaction described in Section 1.3.

Another class of experiments planned at the HRIBF are transfer [e.g., (d, p)] and charge-exchange [e.g., (^{3}He, t)] reactions with radioactive beams. Such reactions have been extensively used with stable beams (e.g., [45]) to indirectly determine stellar reaction rates by populating low energy, near-threshold (p, γ) resonances and measuring resonance energies, spins, and widths. By using radioactive beams, the number of reactions that can be investigated with this technique is greatly expanded. These measurements require higher energies (> 8 - 10 MeV/u) to ensure that the reaction is direct (rather than compound nuclear) and that the reaction products have sufficient energy to be detected. Such measurements can be carried out with, for example, the HRIBF Enge Split Pole Spectrograph. With a beam intensity of 10^9 s^{-1} and a thin target (10^{17} cm^{-2}), 4% statistics can be obtained in a few days for such studies.

Mass measurements, lifetime measurements, and level density determinations will also be made at the HRIBF for nuclei near the proton drip-line that are important for explosive nucleosynthesis processes. Measuring these properties for a few crucial nuclei will help verify the Hauser-Feshbach statistical model programs currently used to estimate many reaction rates involving high-mass ($A > 50$) stable and unstable nuclei. [46]

4 Other Astrophysics Research at ORNL

In addition to the explosive nucleosynthesis measurements described above, there are a number of other astrophysics research efforts at ORNL - in theoretical astrophysics, nuclear astrophysics data evaluation, heavy element nucleosynthesis

measurements, theoretical atomic astrophysics, and atomic astrophysics data. These research programs, some of which are closely coupled to the HRIBF measurement program, are briefly described in the following subsections.

4.1 Theoretical Astrophysics

A new program at ORNL in theoretical and computational astrophysics has as one of its foci the study of stellar explosions and explosive nucleosynthesis. One of the main areas of research is the core collapse supernova mechanism. Simulations in one, two, and three dimensions focusing on issues of neutrino transport, convection, and their interplay in the explosion mechanism are being carried out on supercomputers. In particular, one-dimensional simulations have been conducted using exact Boltzmann neutrino transport to determine whether ν transport approximations have been a primary cause of the *lack* of robust explosions – those that do not rely on finely-tuned parameters – in one or multiple dimensions, both in the presence or absence of convection. [47 - 51] The first multidimensional supernova simulations that implement multigroup transport have also been carried out. [52, 53] Realistic ν transport is crucial for these studies because the explosion mechanism depends sensitively on the ν spectra emerging from the cooling protoneutron star, which ultimately power the explosion. Finally, three-dimensional simulations have been carried out and the development of supernova convection compared with two-dimensional results in an effort to discern any dimensional dependence of supernova convection. [54] Another research effort is also currently under way to model abundance yields in nova explosions; this work is closely coupled to the HRIBF experimental measurement program and to the nuclear astrophysics data work described below.

4.2 Nuclear Astrophysics Data

Computer models of diverse, exciting astrophysical phenomena such as stellar explosions, the early universe, the interstellar medium, and red giant stars require a very diverse set of nuclear physics information to ascertain the rates of and energy released in the relevant nuclear reactions. The rates are derived from laboratory measurements of cross sections of relevant reactions; additionally, information on the properties (e.g., masses, lifetimes, level densities) of the nuclei involved in astrophysical processes are required to calculate unmeasured reaction rates. Astrophysical models have a crucial dependence on the completeness, precision, and timeliness of this input nuclear data. New measurements of crucial reaction rates can, for example, significantly alter model predictions of astrophysical phenomena.

14

A number of projects are underway to meet the nuclear astrophysics data needs of the ORNL experimental and theoretical nuclear astrophysics research programs. For example, to prepare for the HRIBF measurements of the $^{14}O(\alpha, p)^{17}F$ and $^{17}F(p, \gamma)^{18}Ne$ reactions, evaluations of these rates using the most recent indirect experimental measurements of relevant reaction parameters have recently been completed. [55] The $^{14}O(\alpha, p)^{17}F$ evaluation was motivated by the lack of an analytic expression for this rate as a function of temperature in the most recent work. [14] The $^{17}F(p, \gamma)^{18}Ne$ study was motivated by finding a 13 % error in the latest calculation of this rate. [16] Analytic expressions for these two rates were generated in two popular formats – that used in the important Caughlan and Fowler compilation of reaction rates [56], and that used in a more extensive and more recent reaction compilation. [57] Both formats can be readily input into reaction rate network codes. Another project addressed the need to easily (i.e., electronically) incorporate the 160 thermonuclear reaction rates (and their inverses) in the Caughlan and Fowler compilation into computer models. Since this extremely valuable, published compilation of reaction rates has never before been disseminated electronically, these rates have been entered into a computer in the form of a downloadable FORTRAN subroutine and posted on the ORNL Physics Division World Wide Web site. [58] Tabular data for these rates and plots of rates versus temperature are also online. The temperature derivatives of these rates, useful for coupling nucleosynthesis calculations to hydrodynamics, are currently being calculated. Another data project involved compiling a nuclear astrophysics data reference list, that is posted on the World Wide Web. [59] Finally, a fourth data project involved documenting the capabilities that the U.S. nuclear data community can offer to the evaluation of nuclear data of importance to astrophysics [60], as well as helping launch an effort to coordinate U.S. researchers who are addressing nuclear astrophysics data needs.

4.3 Heavy Element Nucleosynthesis Measurements

The elements heavier than Fe are believed to be produced primarily by three processes: in the thermally-pulsing He-shells of low-mass Asymptotic Giant Branch stars via a series of slow neutron capture reactions (and subsequent beta-decays) on Fe seed nuclei, the s-process [61]; in the high-entropy, low-density wind behind the shock wave of a core collapse supernova explosion via a series of rapid neutron capture reactions (and subsequent beta-decays) on Fe seed nuclei, the r-process [62]; and via photodissociation reactions of heavier nuclides, perhaps also in supernovae, the p-process. [63] Models of these processes require as input the accurate rates of neutron capture reactions on a large number of nuclei. Improved rates are required for a number of neutron capture reactions because of the failure of

current nucleosynthesis models to accurately reproduce certain observed abundances. In some cases, the solution may lie with reaction rates that were derived from (n, γ) cross section measurements that were measured with a lower energy limit of 3 keV. This limit is too high to accurately determine the reaction rate at the low temperatures (kT=6-8 keV) advocated by the newest stellar models of the s-process. [61] Furthermore, the lack of neutron transmission data for numerous isotopes prevents the calculation of finite sample-thickness corrections to capture data. The Oak Ridge Electron Linear Accelerator (ORELA) pulsed white neutron source [64] is being used to measure neutron capture and transmission on a number of important s-process isotopes. Recent measurements include: ^{142,144}Nd(n, γ), which gave the first resolution of anomalous Nd abundances in meteorites [65]; ^{134,136}Ba(n, γ), which helped determine the temperature and neutron density of the s-process [66]; ^{116,120}Sn(n, γ), which gave a better understanding of synthesis of Sn isotopes to calibrate the s-process [67]; ^{7}Li(n, γ), which is relevant for the nucleosynthesis of heavy elements in the early universe and for the solar neutrino problem [68]; and ^{137}Ba(n, γ), which demonstrated that resolution of ^{137}Ba abundance anomaly is not caused by low-energy extrapolations of the capture cross section. [69] Measurements in progress include ^{88}Sr(n, γ) and ^{208}Pb(n, γ), and there are plans for measurements of (n, α) reactions relevant to the p-process and for expansion of a high-efficiency array of BaF_2 detectors which would enable the measurement of very small (~mg) samples of separated isotopes. [70] Furthermore, studies of previously unmeasured r-process reactions such as ^{132}Sn(n, γ) will be possible at the HRIBF when neutron-rich radioactive beams become available. With beam intensities of 10^{8-9} s^{-1}, measurements such as ^{132}Sn$(d,p)^{133}$Sn can be made to investigate resonances of importance to the ^{132}Sn(n, γ) reaction.

4.4 Atomic Astrophysics

A newly formed atomic astrophysics theory group at ORNL is actively pursuing a wide range of studies utilizing the most recently available, critically evaluated atomic data. For example, novel spectral modeling of the nebular phase of Type Ia supernovae has lead to an improved constraint on the presently available explosion models, favoring sub-Chandrasekhar mass models, and highlighting the previously discounted role of charge transfer between iron-peak ions and neutrals (see e.g. [71, 72]). Work is also ongoing to model X-ray emission from the Jovian aurora and from comets, and to thereby help determine more accurate physical models of these systems and their interactions. The latter work is also based on the creation and utilization of new databases of atomic collision data, as is a project to extend previous chemical evolution models of the early universe (see e.g. [73]). Study of

16

this chemical evolution reveals the epochs and conditions under which molecules first formed and how they influenced the collapse of early objects through accelerated cooling. These activities are closely coordinated with atomic physics theory and data efforts of the ORNL Controlled Fusion Atomic Data Center. [74]

5 Summary

Measurements of capture reactions on proton-rich radioactive isotopes are crucial to the understanding of explosive nucleosynthesis occurring in spectacular stellar explosions such as novae, supernovae, and X-ray bursts. The Daresbury Recoil Separator has been installed at ORNL's Holifield Radioactive Ion Beam Facility for these measurements. The DRS is currently being commissioned with stable beams, and measurements with proton-rich radioactive beams will begin soon. Initial tests have shown that the DRS can give an excellent suppression of scattered beam particles in inverse kinematics capture reactions. Additionally, development will soon begin on neutron-rich radioactive isotopes relevant for studies of heavy element nucleosynthesis. In addition to the HRIBF measurements, there are astrophysics research efforts at ORNL in theoretical astrophysics and nuclear astrophysics data evaluation which are closely coupled to the HRIBF work, as well as research in heavy element nucleosynthesis, theoretical atomic astrophysics, and atomic astrophysics data.

Acknowledgements

References

1. R.K. Wallace and S.E. Woosley, *Ap. J. Suppl.* **45** (1981) 389.
2. A.E. Champagne and M. Wiescher, *Ann. Rev. Nucl. Part. Sci.* **42** (1992) 39.
3. P. Decrock et al., *Phys. Rev. Lett.* **67** (1991) 808.
4. P. Leleux, *Nucl. Phys.* **A621** (1997) 183c; R.D. Page et al., *Phys. Rev. Lett.* **73** (1994) 3066.
5. R. Cozach et al., *Phys. Letts.* **B353** (1995) 184.
6. J.S. Graulich et al., *Nucl. Phys.* (1997) submitted; W. Galster, this proceedings.
7. K.E. Rehm et al., *Phys. Rev.* **C52** (1995) R460; **C53** (1996) 1950; **C55** (1997) R566.
8. C.E. Rolfs and W.S. Rodney, *Cauldrons in the Cosmos* (Univ. of Chicago Press, Chicago, 1988).
9. L. van Wormer et al., *Ap. J.* **432** (1994) 326.
10. H. Schatz et al., *Phys. Rep.* **294** (1998) 167.
11. L. Buchmann et al., *Nucl. Phys.* **A415** (1984) 93.
12. M. Wiescher et al., *Astron. Astrophys.* **160** (1986) 56.
13. R.E. Williams et al., *Ap. J. Supp.* **90** (1994) 297.
14. K. I. Hahn et al., *Phys. Rev.* **C54** (1996) 1999.
15. M. Leising and D.D. Clayton, *Ap. J.* **323** (1987) 159.
16. A. García et al., *Phys. Rev.* **C43**, (1991) 2012.
17. S. Kubono, private communication (1997).
18. J.G. Ross, Ph.D. thesis, University of Notre Dame (1994).
19. S. Utku, Ph.D. thesis, Yale University (1994).
20. S. Utku et al., *Phys. Rev.* **C** (1997) submitted.
21. X.G. Zhou et al., *Phys. Rev.* **C53** (1996) 982.
22. K.E. Rehm et al., *Bull. Am. Phys. Soc.* **42** (1997) 1640.
23. C.W. Johnson et al., *Ap. J.* **392** (1992) 320.
24. J.N. Bahcall, *Ap. J.* **467** (1996) 475; J.N. Bahcall and M.H. Pinsonneault, *Rev. Mod. Phys.* **64** (1992) 885.
25. J.N. Bahcall, *Neutrino Astrophysics* (Cambridge University Press, New York, 1993).
26. A. Csoto, *Phys. Lett.* **B394** (1997) 247.
27. T. Motobayashi, *Nucl. Phys.* **A621** (1997) 131c; T. Motobayashi, this proceedings.
28. J.D. Garrett et al., *Nucl. Phys.* **A557** (1993) C701.
29. J.B. Ball, *Nucl. Phys.* **A415** (1994) C15.
30. C. Barton et al., private communication (1997).
31. G.D. Alton et al., *Nucl. Inst. Meth.* **A328** (1993) 325.
32. G.D. Alton, *Nucl. Inst. Meth.* **A382** (1996) 207.
33. Alcen^{TM}, Aluma Fiber, RATH Performance Fibers, Wilmington, VA, USA.
34. G.D. Alton and G.D. Mills, *Nucl. Inst. Meth.* **A382** (1996) 232.
35. G.D. Alton and C.L. Williams, *Nucl. Inst. Meth.* **A382** (1996) 237.

36. G.D. Alton, *Nucl. Inst. Meth.* **A382** (1996) 276.
37. H.K. Carter et al., *Nucl. Inst. Meth.* **B126** (1997) 166.
38. G.D. Alton and R. Welton, private communication (1997).
39. J. Görres and M. Wiescher, *Nucl. Inst. Meth.* **B56/57** (1991) 536.
40. M.S. Smith, C. Rolfs, and C.A. Barnes, *Nucl. Inst. Meth.* **A306** (1991) 233.
41. A.N. James et al., *Nucl. Inst. Meth.* **A267** (1985) 144.
42. A.N. James, private communication (1997).
43. L. Gialanella et al., *Nucl. Inst. Meth* **A376** (1996) 174.
44. P.J. Sellin et al., *Nucl. Inst. Meth.* **A311** (1992) 217.
45. M.S. Smith et al., *Nucl. Phys.* **A536** (1992) 333.
46. T. Rauscher, F.-K. Thielemann, K.-L. Kratz, *Nucl. Phys.* **A621** (1997) 331c.
47. A. Mezzacappa and S.W. Bruenn, *Ap. J.* **405**, (1993) 637.
48. A. Mezzacappa and S.W. Bruenn, *Ap. J.* **405**, (1993) 669.
49. A. Mezzacappa and S.W. Bruenn, *Ap. J.* **410**, (1993) 740.
50. A. Mezzacappa, in *Proceedings of the 18th Texas Symposium on Relativistic Astrophysics* (1997) in press.
51. O.E.B. Messer et al., *Ap. J.* (1998) submitted.
52. A. Mezzacappa et al., *Ap. J.*(1998) in press.
53. A. Mezzacappa et al., *Ap. J.* (1998) in press.
54. J.M. Knerr et al., *Ap. J.* (1998) submitted.
55. D.W. Bardayan and M.S. Smith, *Phys. Rev.* **C56** (1997) 1647.
56. G.R. Caughlan, W.A. Fowler, *At. Data Nucl. Data Tables* **40**, (1988) 283.
57. F.-K. Thielemann et al., Adv. Nucl. Asto. 525 (1987); Ch. Freiburghaus and F.-K. Thielemann (1995): http://isotopes.lbl.gov/isotopes/astro/friedel.html.
58. ORNL Nuclear Astrophysics Data Website: http://www.phy.ornl.gov/astrophysics/data/data.html.
59. P.D. Parker et al., (1996): http://isotopes.lbl.gov/isotopes/astro/astroref.html.
60. M.S. Smith et al., U.S. Nuclear Reaction Data Network Astrophysics Task Force Report (1995): http://www.dne.bnl.gov/~burrows/usnrdn/astrodata.html.
61. O. Straniero et al., *Ap. J.* **440** (1995) L85.
62. S. Woosley et al., *Ap. J.* **433** (1994) 229.
63. M. Rayet et al., *Astron. Astophys.* **298** (1995) 517.
64. R.L. Macklin and B.J. Allen, *Nucl. Inst. Meth.* **91** (1971) 565.
65. K.H. Guber et al., *Phys. Rev. Lett.* **78** (1997) 2704.
66. P.E. Koehler et al., *Phys. Rev.* **C54** (1996) 1463.
67. P.E. Koehler et al., *Bull. Am. Phys. Soc.* **42** (1997) 983.
68. J.C. Blackmon et al., *Phys. Rev.* **C54** (1996) 383.
69. P.E. Koehler et al., *Bull. Am. Phys. Soc.* **42** (1997) 1680.
70. K.H. Guber et al., *Nucl. Phys.* **A621** (1997) 254c.
71. W. Liu, D.J. Jeffery, and D.R. Schultz, *Ap. J.* **483** (1997) L107.
72. W. Liu et al., *Ap. J.* **489** (1997) L141.
73. P.C. Stancil, S. Lepp, and A. Dalgarno, *Ap. J.* **458** (1996) 401.
74. ORNL Controlled Fusion Atomic Data Center: http://www-cfadc.phy.ornl.gov/.

19

Report Number (14) ORNL/CP--96139
CONF-971115--

Publ. Date (11) 199712
Sponsor Code (18) DOE/ER, XF
JC Category (19) UC-400, DOE/ER

DOE